Titanium Sapphire Laser

Julien Samson-Kornik, 05230449 Submitted for Evaluation on December 18, 2018

Contents

1 History and Applications

The Titanium Sapphire (Ti:Al_2O_3, or Ti:Sapphire) laser was developped in the quest for tunable solid state lasers [14] and was first demonstrated by P.F. Moulton at Lincoln Laboratory in 1982. The discovery was possible due to the availability of laser quality Titanium-doped Sapphire crystals, grown using the "seeded vertical-gradient freeze method", a technique also demonstrated at Lincoln Labs, in 1977 [11]. It was subsequently discovered that the Titanium Sapphire laser could be mode-locked by a phenomenon known as Kerr Lens Mode Locking [14], and pulses as short as 45 fsec had been generated by 1990 [8].
A revolution in the amplification of short pulses came in 1985, when Chirped Pulse Amplification (CPA) was demonstrated on an Nd-YAG laser [1] to generate picosecond pulses at the millijoule level. In 1998, the technique of CPA, in combination with a mode locked Ti:Sapphire laser were then used at the Lawrence Livermore National Laboratory to seed pulses with a peak power exceeding 1.50 PW [15], which can be used for high-energy physics research [2] and for soft X-Ray laser pumping which can be used for biological imaging [15]. In addition to the applications listed above, pulse Ti:Sapphire lasers have been used as Optical Frequency Combs, which can be used to measure the separation between optical frequencies. The Nobel prize in physics of 2005 was awarded for the development of the optical frequency comb.

2 Gain Medium

The electronic structure of Ti^{3+} is a closed shell plus a single 3d electron [9]. In free-space, the d-electron orbitals are fivefold degenerate but when when a small amount of aluminum ions of the host medium are substituted for Ti^{3+} ions, the degeneracy is split by the cubic crystal field [2]. This difference in energy between the otherwise degenerate states can be intuitively understood by noting that in the T state the orbitals do not point directly at the neighboring Oxygen atoms while in the E state they do. This splitting, which amounts a wavelength difference in the visible spectrum at around 19000 $cm^{-1} \approx 526$ nm (green) [9], is shown diagrammatically in Fig. 5:

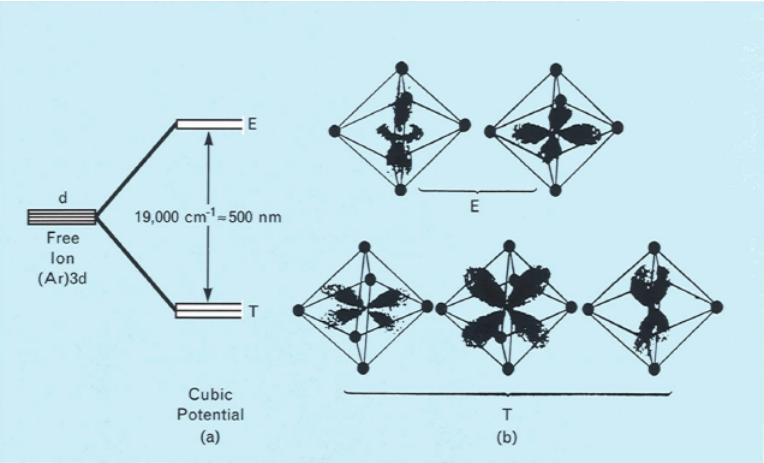

Figure 1: Left: Energy diagram showing splitting of the 3d electron states to the E and T levels. Right: Probability distribution of the electron in the T and E states. [2]

This coupling between the Ti^{3+} states and the crystal can also be used to to gain an intuition for mechanisms behind the large bandwidth of the emission spectrum; a decay from an excited E state to a T state will be stokes shifted and acompanied by phonons due to the coupling with the neighboring oxygen atoms [2]. In more precise terms, the ^2E state is split due to a the presence of a lower energy state which can be attained with a shift in position of the Ti^{3+} ion relative to the 6 Adjacent Oxygen atoms [2]. This is known as the the Jahn-Teller effect and it results in two Gaussian levels with a separation of 1850 cm^{-1}. The degenerate $^2T_2$ state is also split into 2 levels, with the lower of the levels split by by the spin-orbit interaction. After the stokes shifted emission occurs, additional vibrational excitations will again occur as

the Ti^{3+} shifts back to it's lower energy configuration. This coupling to the crystal field, in combination with the fact that higher energy levels are effectively inaccessible, results in what is effectively 4-level laser system [1]. A diagrammatic representation is shown below, in Fig 2:

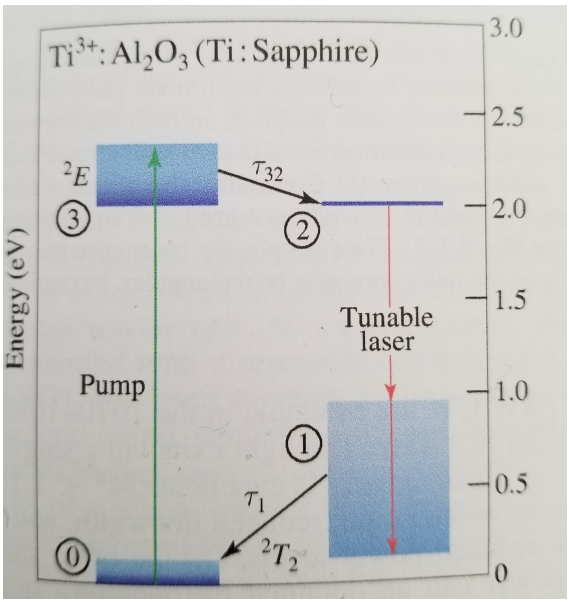

Figure 2: Ti:Sapphire as a 4-level laser system, along with the relative widths of the energy levels [16]

The linewidths of each energy level in combination with the vibronic transitions contribute to a bandwidth which spans ~ 5000 cm^{-1}, the largest of any of the paramagnetic ion lasers that were developed as of the invention [7]. This is the reason for the broad tunability as well as the potential to generate extremely short pulses. The absorption and gain profiles are shown in Fig. 3.

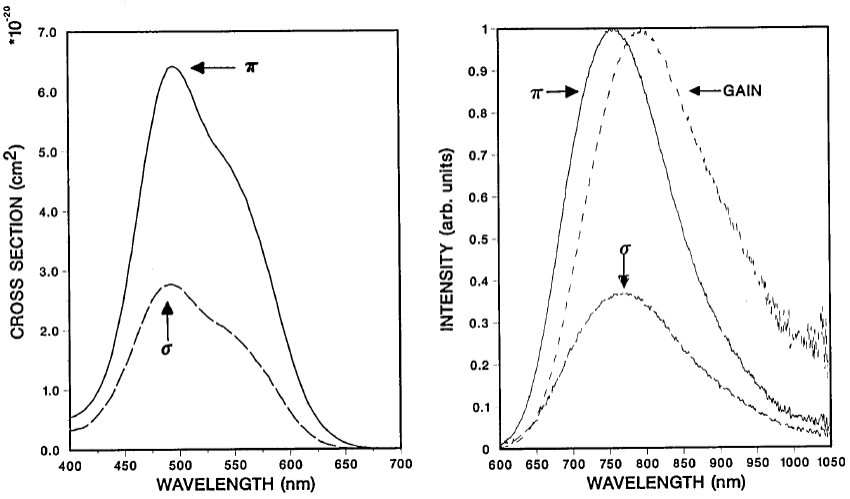

Figure 3: Left: Absorption cross section as a function of $\pi$and σ polarization. Right: Intensity and polarization dependent emission profile. Image taken from [9].

[1] A complete theoretical treatment of Ti^{3+} impurities in Al_2O_3 is given in [18].

3 Operation

3.1 Pumping

Performance of the Ti:Sapphire laser is improved upon using a laser pump rather than a flash-lamp. Some sources ([17]) quote the $\sigma\tau$ product, which is equal to 1.1 $\times 10^{-24}$ $cm^2 s$ along with the relatively high losses as the reason laser pumping is preferable. The improved performance that is achieved via laser pumping can also be understood by noting that both the fluorescence lifetime and the absorption cross section are small. The fluorescence lifetime at room temperature is equal to $\tau = 3.115 \pm 0.05$ μ sec [9] and the absorption cross section is 3.5 $\times 10^{-19}$ cm^2 at the peak. These factors in combination with the polarization dependent absorption (Fig. 3) make controllable, high flux pumping favorable. A diagram showing the fluorescence lifetime as a function of temperature is shown in Fig. 4.

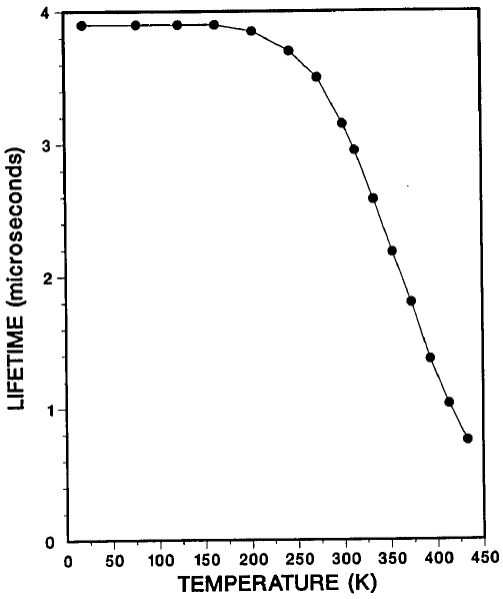

Figure 4: Fluorescence Time as a function of Temperature. The fast decay with increasing temperature is thought to be due to an increase in multi-phonon nonradiative decay [9].

Due to these factors and an absorption band that peaks in the green region of the spectrum, its pumping is best accomplished using an Argon-Ion [8] or frequency doubled Nd:YAG [6] laser. Pulsed operation as well as tunable CW operation can be achieved using Ti:Sapphire, however this paper is restricted in scope to pulsed operation.

3.2 Pulsed

This section will focus on Passive Mode Locking, however Ti:Sapphire lasers have been model locked using a variety of techniques, including [8]:

- Synchronous Pumping
- Acousto-Optic Mode Locking
- Passive Mode Locking
- Injection Seeding
- Coupled-Cavity Mode Locking

Injection Seeding and Coupled-Cavity Mode Locking have achieved pulse durations of 300 fsec and 800 fsec, respectively. Passive Mode Locking has achieved 2 psec pulses and is limited by Group Velocity Dispersion however, intracavity dispersion compensation has been used in conjunction with the passive technique of Kerr Lens Mode Locking (KLM) to generate pulses as short as 60 fsec in duration. The configuration for this strategy is shown below:

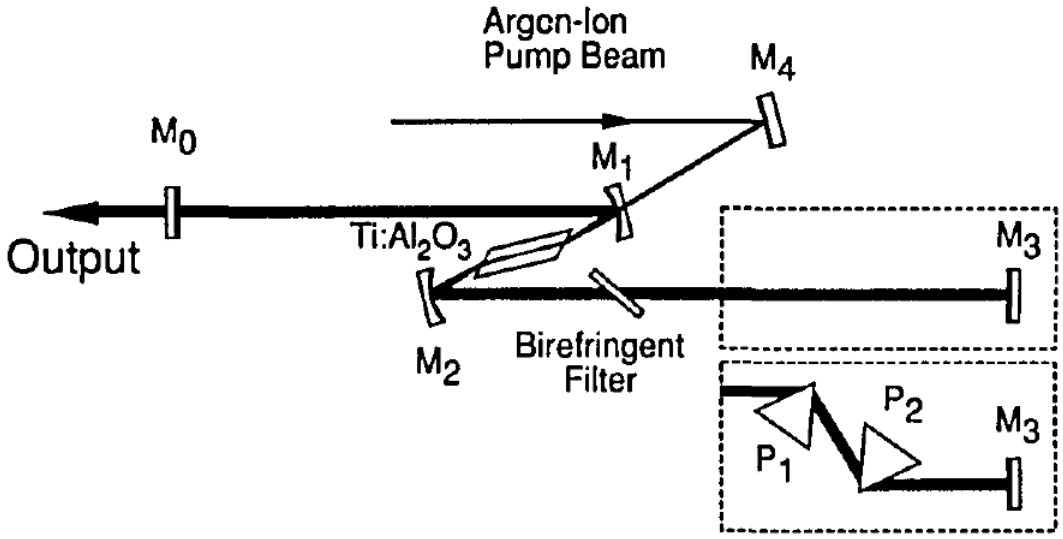

Figure 5: Kerr Lens Mode Locking with Intracavity Dispersion Compensation [8]. The authors of this article noted KLM for this experiment had to be started by making small realignments to the cavity mirrors, but the effect was passive otherwise.

A further reduction in pulse duration to less than 50 fsec has been achieved using extracavity pulse compression techniques to provide adjustable anomalous group-velocity dispersion.

Kerr Lens Mode Locking is a process wherein an intensity dependent refractive index in combination with an aperture is used to filter out low intensity signal while preserving the high-intensity part. This effect can be understood intuitively by considering that the the gain medium has a high bandwidth, the cavity will then support many-modes as well. The summation of the electric-field of the many modes will produce an amplitude modulation that is dependent on the phase-difference between the modes, because this is random, at some points in time there will be a low modulation depth and at some points there will be a high-modulation depth, the combination of an intensity-dependent focusing and an aperture will conserve the portions of the beam who's phases add constructively while filtering out the the ones that do not. In practice the filtering of the low-intensity portion of the beam is not always done by an aperture but by applying perturbations to the laser system [8], this can be attributed to induced instabilities to the laser resonator which will cause the low intensity wings of the beam to be filtered out. An illustration of KLM is shown in Fig. 6.

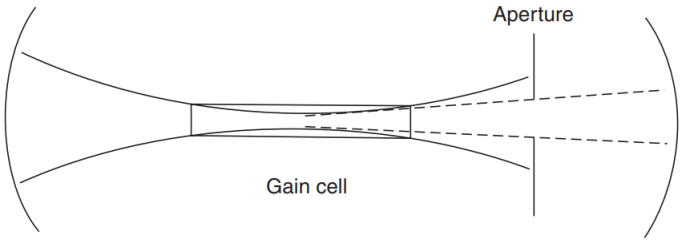

Figure 6: In KLM the low-intensity portion of the beam is filtered out, leaving only high-intensity (mode locked) portions of the beam. Image taken from [10, p.532].

Pulsed lasers can also be used to produced high intensity pulses, an important application of the Ti:Sapphire laser. A major breakthrough occurred in 1985 when the technique of Chirped Pulse Amplification (CPA) for optical pulses was demonstrated [13]. This technique is similar to the group velocity dispersion compensation discussed earlier, however in this technique the pulse is deliberately stretched before amplification in order to increase the energy of the pulse without increasing the intensity to levels that would damage the components of the system. The pulse is then compressed to achieve the high peak intensity. This technique is shown diagrammatically in Fig. 7.

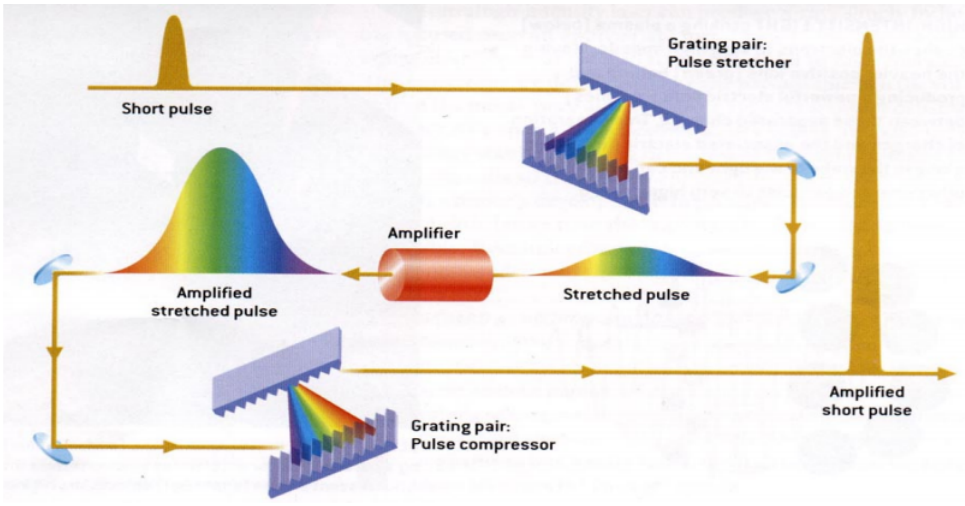

Figure 7: Illustration of the steps involved in CPA [13]. A short high intensity pulse is stretched below the damage threshold of the system using a grating pair, amplified and then re-compressed.

The first implementation was accomplished using pulses produced by a Mode-Locked Nd:Yag laser. The pulses produced were linearly chirped by the combination of group velocity dispersion and self-phase modulation through a 1.4 km fiber. Then, the pulse was amplified through Nd:glass, the pulse is passed through the regenerative amplifier a fixed number of times via a Pockels cell. The pulse is then compressed using a double grating compressor. A sketch of the experimental configuration used to first demonstrate this process is shown in Fig. 8, which succeeded in producing 2 ps pulses with energies at the millijoule level.

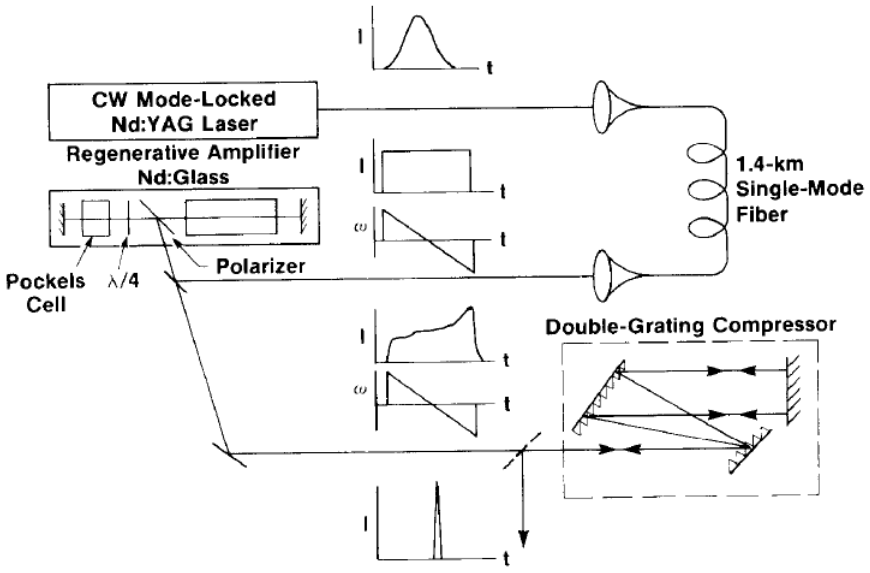

Figure 8: Experimental setup used by Strickland and Mourou to demonstrate CPA [13].

This technique can also be applied to Ti:Sapphire, which has a significantly larger bandwitdth than the Nd:YAG used by Strickland and Mourou. In combination with additional developments this method has used to develop a KiloJoule, Petawatt Ti:Sapphire based laser at Lawrence Livermore National Laboratory [15].

4 Applications: Optical Frequency Metrology

Wavelength measurement techniques are limited in precision to a few parts in 10^{10} by wavefront errors [4]. To overcome this limitation, frequency measurements were first performed using large harmonic frequency chains, but these had to be specifically engineered for the problem at hand and were highly intricate [4]. Many other methods of optical frequency measurements have since been tried but as of 1998 were supplanted with femtosecond laser optical frequency combs [4], which essentially serve as a ruler for measuring frequency. In a femtosecond frequency laser comb, a mode-locked broadband pulse laser is used to generate a sequence of pulses that are superimposed (heterodyned) with the source who's frequency is to be measured. The frequency is then inferred by measuring the beat frequency between the comb and the CW source, which is substantially down shifted from the original by the process. As long as the spectrum of the comb is known, then the frequency of the CW source can be deduced. To understand the process, first consider the general mathematical form of a pulse train, shown in Eq. 1:

$$\text{Ш}(\frac{t}{T}) * E_1(t), \tag{1}$$

where T is the pulse repetition period, which translates to pulse repetition frequency

$$f_r = \frac{1}{T} = \frac{\nu_g}{2L}, \tag{2}$$

Where, ν_g is the group velocity of the pulse [21] and $E_1(t)$ denotes the electric field of a single pulse. In the frequency domain, Eq. 1 corresponds to a comb with frequency spacing given by Eq. 2, modulated by the spectrum of the pulse [25, p.222]:

$$\text{Ш}(\frac{f}{f_r})E_1(f) = \sum_n E_1(nf_r)\delta(f - nf_r). \tag{3}$$

Another way to think of this is to consider the modes of the cavity in a standing wave picture, which are again given by Eq. 2, which form a comb in the frequency domain [2], this comb, in combination with the wide gain profile of the titanium-doped sapphire [3] will produce a spectrum in the form of Eq. 3. In practice however, there is an additional offset phase f_o introduced by the comb, and the nth comb line is actually given by:

$$f_n = nf_r + f_o, \tag{4}$$

where f_o results from the phase-difference between the pulse envelope and carrier (see [10, eq. 14.7.23-24] for a derivation). The frequency comb, shown in Eq. 3, now has the form:

$$\sum_n E_1(nf_r)\delta(f - nf_r + \Delta\phi) \tag{5}$$

[2]The Finesse of the cavity will of course limit the sharpness of the comb but has not been considered here and can be assumed to be high.

[3]The comb used in a precision measurement of the Cesium D_1 line and the fine structure constant used a span of 244 000 modes [21] and combs with a span of 10^6 modes are possible [22].

This is shown graphically in Fig. 9, where the time domain and frequency domain representations are both shown.

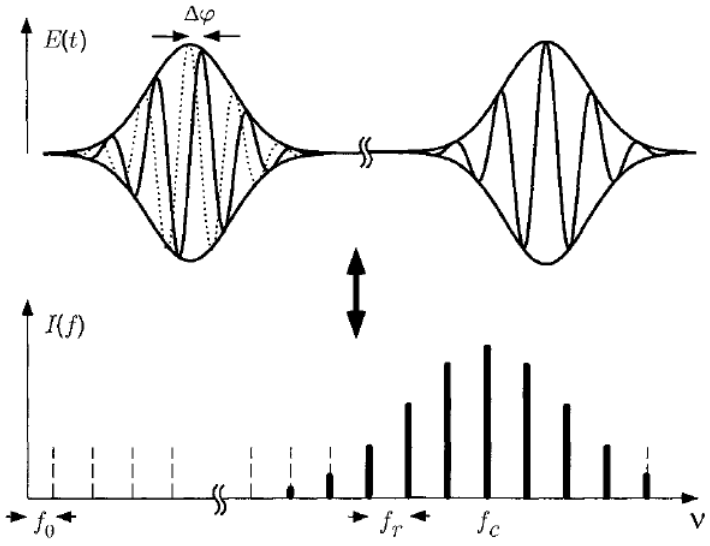

Figure 9: Top: Time Domain representation of pulsed laser. Bottom: Frequency Domain (magnitude squared) representation, showing combination of pulse spectrum with the comb line, as well as the repetition frequency f_r and the offset frequency f_o [21].

In theory, the offset frequency can be measured by frequency doubling the lower end of the spectrum to $2f_n$ and measuring the beat frequency with the upper end at frequency f_{2n} using a photo-detector [22], which directly provides the offset frequency. This process is illustrated diagrammatically in Fig. 10.

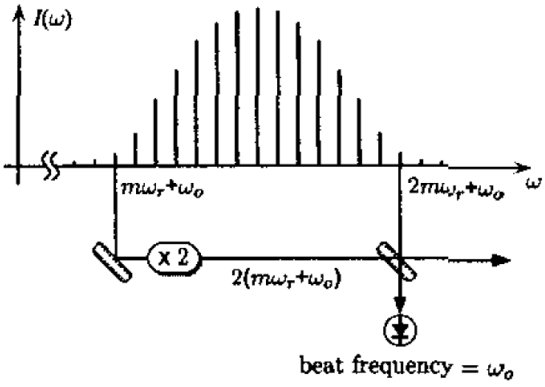

Figure 10: Frequency Spectrum representation of measurement of offset frequency $\omega_r = 2\pi f_r$ [20].

To achieve this octave-spanning spectrum, the femtosecond pulse spectrum is broadened via self-phase modulation in an optical Photonic Crystal Fiber (PCF) [22]. To achieve this nonlinear effect, the beam is tightly focused within the central region of the optical fiber core shown in Fig. 11 to achieve a high intensity. The air holes around the central region allow the pulse to remain tightly focused and reduce effects of group velocity dispersion [4].

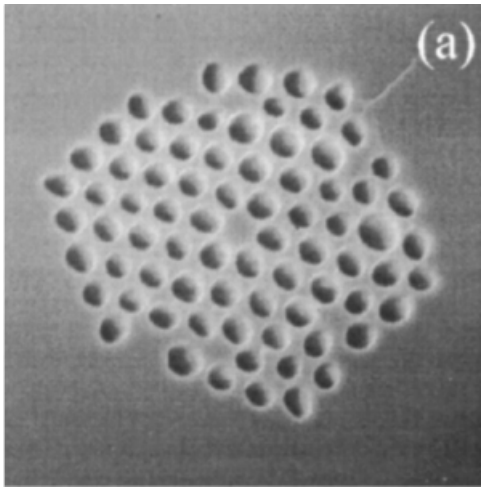

Figure 11: A Photonic Fiber, from [26].

The high intensity beam increases the nonlinear effect because the frequency broadening occurs due to the non-linear refractive index of the medium which is proportional to the intensity through $n(t) = n_0 + n_2 I(t)$, this causes a time-dependent phase-shift which in turn broadens the pulse [27, p. 376].

The pulses are then split into high and low frequency components using a dichroic mirror. The "Infrared" (low frequency) end of the spectrum is doubled using a KTP crystal and recombined with the already "green" (high frequency) end of the spectrum, the beam is then filtered and the beat frequency is recorded. This is shown schematically in Fig. 13.

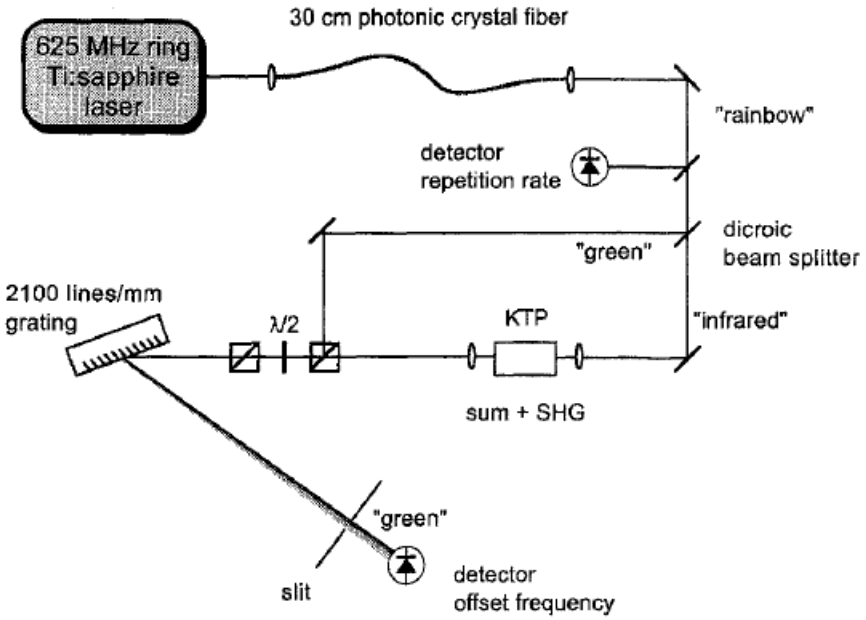

Figure 12: Schematic of experimental setup for measurement of the offset frequency [21].

A physical setup for generating optical an optical frequency comb is shown in Fig. 13.

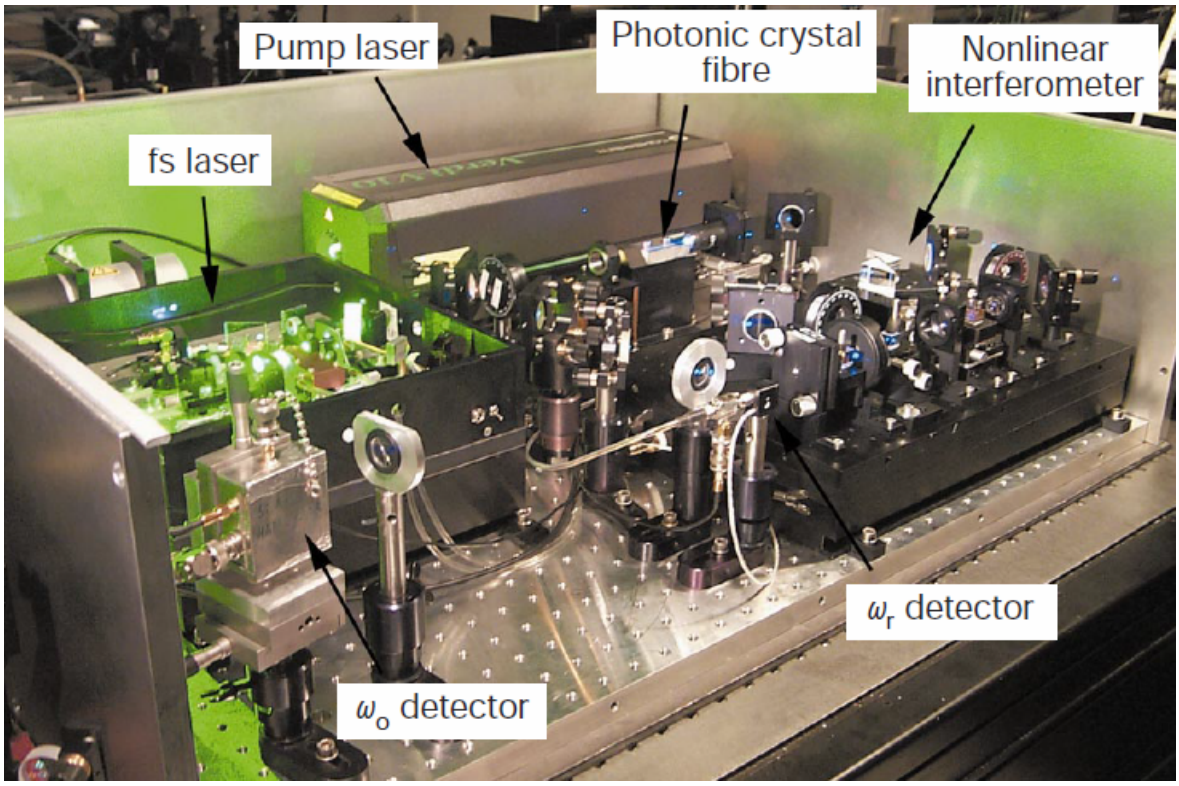

Figure 13: Optical Frequency Synthesize, showing Pump, Pulsed Laser, photonic crystal fiber (Fig 11) and apparatus for measuring f_r and $\Delta\phi$ [22].

The determination of the frequency of an unknown source is performed in a fashion similar to the determination of the offset phase. It is inferred from the interference between the pulse laser and the unknown source; a low frequency beat-note is produced whenever a comb line is close to the frequency of the unknown source. When this beat-note occurs, as long as n, f_r and $\Delta\phi$ from Eq. 5 can be determined then this beat note can be related to the frequency of the unknown source. The pulse repetition frequency f_r can be determined by heterodyning with source of known frequency, such as a Cesium atomic clock, and n can be determined with a wave-meter.

References

[1] D. Strickland, G. Mourou, Compression of Amplified Chirped Optical Pulses, Optics Communications, Volume 56, number 3, 1 December 1985.

[2] K.F. Wall, A. Sanchez, Titanium Sapphire Lasers, The Lincoln Laboratory Journal, Volume 3, Number 3, 1990.

[3] R.R. Joyce, P.L. Richards, Far-Infrared Spectra of Al2O3 Doped with Ti, V and Cr, Lawrence Berkeley National Laboratory, 1968-06-01.

[4] T.W. Hansch, Nobel Lecture: Passion for Precision, Reviews of Modern Physics, Vol. 78, 17 November 2006.

[5] X. Ding et al., High Power Widely Tunable Narrow Linewidth All-Solid-State Pulsed Titanium-Doped Sapphire Laser, Chin. Phys. Lett., Vol. 28,. No. 9, 2011.

[6] L.G. DeShazer, G.F. Albrecht, J.F. Seamans, Tunable Titanium Sapphire Lasers, Pric. SPIE 0622, High Power and Solid State Lasers, 23 June 1986.

[7] P.F. Moulton, Survey of Tunable Solid State Lasers, Proc. SPIE 0622, High Power and Solid State Lasers, 23 June 1986.

[8] D.E. Spence, P.N. Kean, W. Sibbett, 60-fsec pulse generation from a self-mode-locked Ti:sapphire laser, Optics Letters, Vol.16,No.1,January 1, 1991.

[9] P.F. Moulton, Spectroscopic and laser characteristics of Ti:Al_2O_3, Opt, Soc. Am. B., Vol. 3, No. 1, January 1986.

[10] Peter W. Milonni, Joseph H. Eberly. "Laser Physics", Wiley, 2010.

[11] T.B. Reed, R.E. Fahey, P.F. Moulton, Growth of Ni-Doped MgF_2 crystals in self-sealing graphite crystals, Journal of Crystal Growth 42, 1977.

[12] P.F. Moulton, Titanium-Dope Sapphire Laser Research and Design Study, NASA Contract Report 4093, September 1987.

[13] Advanced information. NobelPrize.org. Nobel Media AB 2018. Sat. 3 Nov 2018. ¡https://www.nobelprize.org/prizes/physics/2018/advanced-information/¿

[14] SPIETV. "Peter Moulton on the Ti:Sapphire Laser", YouTube, 27 Aug. 2010, www.youtube.com/watch?v=D4Ej0k6z_fc.

[15] M. D. Perry et. al., "Petawatt laser pulses", Optics Letters, Vol. 24, No. 3, February 1, 1999.

[16] Saleh, Bahaa E. A., Teich, Malvin Carl. "Fundamentals of photonics", Wiley-Interscience, Second Edition

[17] H. Jelinkova et. al., "Pumping of Titanium Sapphire Laser", Czechoslav Journal of Physics, Vol. 43, No. 2, 1993.

[18] R.M. MacFarlane, J.Y. Wong, M.D. Sturge, "Dynamic Jahn-Teller Effect in Octahedrally Coordinated Impurity Systems", Physical Review, Vol. 166, No. 2, 10 February 1968.

[19] D.J. Jones, S.A. Diddams et. al., "Carrier-Envelope Phase Control of Femtosecond Mode-Locked Lasers and Direct Optical Frequency Synthesis", Science, Vol. 288, 28 April 2000.

[20] T. Udem et. al., "Measuring the Frequency of light with a Mode-Locked Laser", IEEE, 2002.

[21] R. Holzwarth, "Optical frequency metrology and its contribution to the determination of fundamental constant", AIP Conference Proceddings 551, 58, 2001.

[22] T. Udem, R. Holzwarth, T.W. Hansch, "Optical Frequency Metrology", Nature, Vol. 416, 14 March 2002.

[23] R. Pohl et. al., "The size of the proton", Nature, Vol. 466, 8 July 2010.

[24] S. Diddams, KISSCaltech, "Fundamentals of frequency combs: what they are and how they work", Youtube, 10 Nov 2015, https://www.youtube.com/watch?v=njtHAxqo7bU.

[25] Bracewell, Ronald N. The Fourier Transform and Its Applications. New York :McGraw-Hill, 2000. Third Edition.

[26] J.K. Ranka, R.S. Windeler, A.J. Stentz, "Visible continuum generation in air-silica microstructure optical fibers with anomalous dispersion at 800 nm", Optics Letters, Vol. 25, No.1, January 1, 2000.

[27] R.W. Boyd, Nonlinear Optics, Academic Press, Third Edition.